FULL PAPER

ADVANCED FUNCTIONAL MATERIALS

Short-Time Tuning of the Biological Activity of Functionalized Polyelectrolyte Multilayers**

By *Nadia Benkirane-Jessel*, *Philippe Lavalle*, *Eric Hübsch*, *Vincent Holl*, *Bernard Senger*, *Youssef Haïkel*, *Jean-Claude Voegel*, *Joëlle Ogier*, and *Pierre Schaaf**

This article demonstrates the tuning of the biological activity of a surface functionalized by a polyelectrolyte multilayer. The interaction of protein A with macrophages is used as the model system. The film consists of two polypeptides, poly(lysine) and poly(glutamic acid); each "build-up" solution is a mixture of the respective D- and L-enantiomers (*d* and *l* enantiomers). Cells are deposited on top of the film, and they produce tumor necrosis factor alpha (TNF-α) as they come into contact with the protein. Depending upon the *d*/*l*-enantiomer ratio of the polyelectrolyte solutions used for the film build-up, and the embedding depth of the protein, the production of TNF-α commences after a varying induction time and displays a transition from no-production to full-production, which takes place over a period of time that depends on the film's composition and embedding depth. Thus, it is shown that by changing these two parameters the timing of the protein's activity can be accurately tuned.

1. Introduction

Over the past years, much effort has been devoted to rendering materials biologically active. The first trials were aimed at providing them with a single functionality. For example, coronary stents coated with heparin present antithrombotic properties,[1] or, coated with an anti-proliferative agent, such as rapamycin, reduce restenosis.[2] Different methods have been developed to achieve this aim: active molecules were incorporated directly into the material,[3–5] or were fixed on the surface of the material merely by adsorption[6,7,8] or chemical grafting.[9–11] Bioactive molecules, such as insulin[12] or epidermal growth factor,[13] have, for example, been chemically grafted and immobilized on surfaces. None of these methods is, however, free of drawbacks: incorporating active molecules into the bulk of a given material is not always possible; the adsorption of molecules often involves weak bonds, so that the molecules rapidly desorb, and chemical grafting can be very difficult to achieve. Moreover, the irreversible attachment of molecules to a surface may also reduce their biological activity. A second generation of bioactive materials presenting time-scheduled activity and multifunctionalization is now under development. Recently, Langer and co-workers reported biodegradable polymeric microchips that release pulses of active molecules with a precision of a few days over a period of five months.[14] These chips consist of macroscopic reservoirs filled with the active molecules, and closed by a biodegradable poly[(D,L-lactic acid)-*co*-(glycolic acid)] membrane.

Depositing polyelectrolyte multilayers on charged surfaces offers a new route to functionalized biomaterials.[15] These coatings are obtained by alternately dipping a charged surface in polyanionic and polycationic solutions. The simplicity and versatility of such a build-up procedure creates great possibilities for its widespread use in biomaterial coating. We have recently equipped polyelectrolyte multilayers with anti-inflammatory properties by incorporating anti-inflammatory drugs or peptides into the film architectures.[16–18] Bioactive proteins can also be directly integrated in the architecture without any covalent bonding with a polyelectrolyte, retaining a secondary structure close to that of their native form.[19–25] Partially degradable layered structures could thus be advantageous for the progressive delivery of associated active agents.

Recently, we demonstrated that cells were able to react with protein A (PA) embedded in poly(L-glutamic acid)/poly(L-lysine) (P*l*GA/P*l*L) multilayer architectures.[19] This protein, issued from the cell walls of *Staphylococcus aureus*, possesses the ability to bind the fragment c (Fc) of immunoglobulin G (IgG), and also has a large range of biological activity: It acts as an antitumoral,[26,27] antitoxic,[28] anticarcinogenic,[29] anti-

[*] Prof. P. Schaaf, E. Hübsch
Institut Charles Sadron (CNRS/ULP)
6 rue Boussingault, F-67083 Strasbourg Cedex (France)
E-mail: schaaf@ics.u-strasbg.fr
Dr. N. Benkirane-Jessel, Dr. P. Lavalle, Dr. B. Senger, Prof. Y. Haïkel, Dr. J.-C. Voegel, Prof. J. Ogier
Institut National de la Santé et de la Recherche Médicale, Unité 595, Faculté de Chirurgie Dentaire, Université Louis Pasteur
11 rue Humann, F-67085 Strasbourg Cedex (France)
Dr. V. Holl
Institut de Virologie, UPRES EA 3770, ULP
1 rue Koeberlé, F-67000 Strasbourg (France)

[**] This work was supported by the Ligue contre le Cancer (Région Alsace). N.J. is indebted to the Faculté de Chirurgie Dentaire of Strasbourg for financial support. The authors are indebted to Marion Dussaussois and Géraldine Greiner for their contribution to the QCMD measurements. The authors also thank Jerôme Mutterer (Institut de Biologie Moléculaire des Plantes, Strasbourg, France) for assistance with the CLSM. The CLSM platform used in this study was co-financed by the Région Alsace, the CNRS, the Université Louis Pasteur, and the Association pour la Recherche sur le Cancer. This work was supported by the program ACI "Nanosciences" (NR204) from the Ministère Français Déligué à la Recherche.

  DOI: 10.1002/adfm.200400129

ADVANCED FUNCTIONAL MATERIALS

fungal,[30] and antiparasitic agent.[31] Furthermore, PA stimulation of the human macrophages leads to the rapid expression of both the pro-inflammatory cytokine tumor necrosis factor alpha (TNF-α) and the anti-inflammatory cytokine IL-10.[32] We examined the effect of the embedding depth of PA in $(P\mathit{l}GA/P\mathit{l}L)_n$ multilayers on its activity by measuring the amount of TNF-α produced by cells grown on these films. We found that cells interact with PA incorporated in polyelectrolyte multilayer films, and showed that they come in contact with the active protein by degrading the film. Values of TNF-α production obtained after 4 h and one night of cell interaction with the films were similar, whatever the embedding depth of protein A (up to $n = 30$), and were comparable to the value obtained when PA was adsorbed on the terminating layer. Finally, we have shown that the replacement of P*l*L by P*d*L forms a barrier that prevents cellular communication with embedded PA.[19]

It has also been recently demonstrated that polyelectrolyte multilayers can be built using polyanionic and/or polycationic mixtures instead of one-component solutions.[33–36] In this case, the two polyelectrolytes form a mixture and are incorporated simultaneously into the multilayer during each deposition step. This leads to new film properties that lie between the extreme properties obtained with the one-component polyelectrolyte solutions. These properties can be tuned by changing the mixing ratio of the polyelectrolytes in the mixture.[35,36] Using the fact that embedding PA in a film composed of D-polypeptides enantiomers completely extinguishes the biological activity of the film, whereas full activity is obtained with L-enantiomers,[19] we will show in this article that the biological activity of the film can be tuned in time by using poly(lysine)/poly(glutamic acid) multilayers constructed with polyanionic and polycationic solutions consisting of *d*- and *l*-mixtures with different *d*//*l* content ratios. Because the *l*- and *d*-enantiomers have the same chemical nature, it is difficult to determine the *d*//*l* ratio present in the film after deposition. This, however, is not the central issue of our paper and will not be addressed here. We used PA and macrophages as the model system, as in our earlier work.[19] The biological activity was followed by measuring the production of TNF-α.

2. Results and Discussion

2.1. Confocal Microscopy Observations

Confocal laser scanning microscopy (CLSM) allowed us to demonstrate that the macrophages develop pseudopods along the film, and that they come into contact with PA, even though it is embedded under twenty pairs of (P*l*GA/P*l*L) layers (Fig. 1). In previous experiments, we could visualize pseudopods developing through the multilayer down to the PA layer.[19] The direct interaction of PA and the cells is further demonstrated here by the fact that the cells become red due to the Texas-Red-labeled PA (Fig. 1c). The progressive degradation of the $(P\mathit{l}GA/P\mathit{l}L)_n$ film as a function of contact time with the cells is visualized in Figures 2a–c. One observes, in particular, the presence of holes in the $(P\mathit{l}GA/P\mathit{l}L)_n$ film, whereas no holes were found in the $(P\mathit{d}GA/P\mathit{d}L)_n$ film after one night of contact of the film with cells (Figure 2d).

2.2. Build-up of Multilayer Films

As already mentioned, we used P*l*GA and P*l*L as degradable polyelectrolytes and P*d*GA and P*d*L as non-degradable polyelectrolytes. The $(PL/PGA)_n$ films were grown using P*d*GA/P*l*GA and P*d*L/P*l*L mixtures containing similar *d*//*l* ratios. These ratios were varied from one construction to another. The PA molecules were embedded at different depths inside these architectures. The multilayered films were constructed by dipping a glass coverslip alternately into the poly(lysine) and poly(glutamic acid) solutions containing the appropriate amounts of the *d*- and *l*-forms of the polyelectrolytes. The total polyanion and polycation concentration was kept fixed at 1 mg mL^{-1} and the *d*//*l* ratio was varied from 0 to 100 %. A film corresponding to *x* % of *d* was thus constructed using a mixture of a poly(lysine) solution containing *x* % of P*d*L and (100–*x*) % of P*l*L with a poly(glutamic acid) solution containing similarly *x* % of P*d*GA and (100–*x*) % of P*l*GA. We first verified that the multilayer build-up was possible for any value of *x* between 0 and 100 %. To this end, film constructions corresponding to

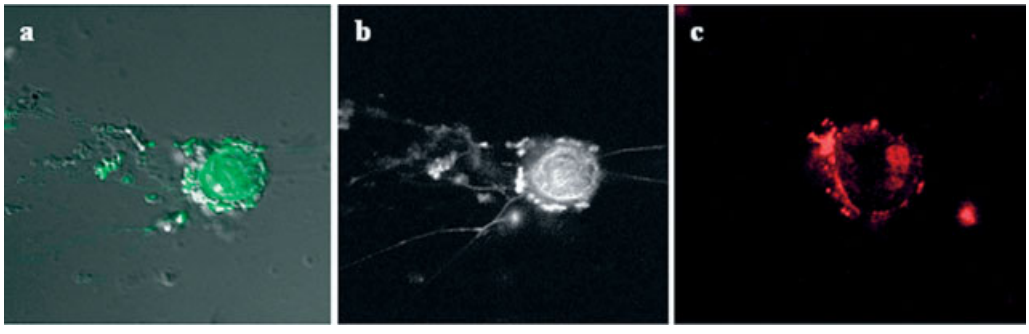

Figure 1. Confocal laser scanning microscopy images of macrophages after 20 min contact with a multilayer film containing PA embedded under twenty pairs of (PlGA-PlL) layers: a) phagocytosis of poly(L-lysine) labeled with fluorescein isothiocyanate, $P\mathit{l}L^{FITC}$, by the cell; and b) pseudopod formation by the cell. c) Cells in contact with a multilayer film containing PA^{TR} (TR: Texas Red) embedded under twenty (PlGA-PlL) pairs of layers after overnight (15 h) contact. Image size = 48.7 μm × 48.7 μm.

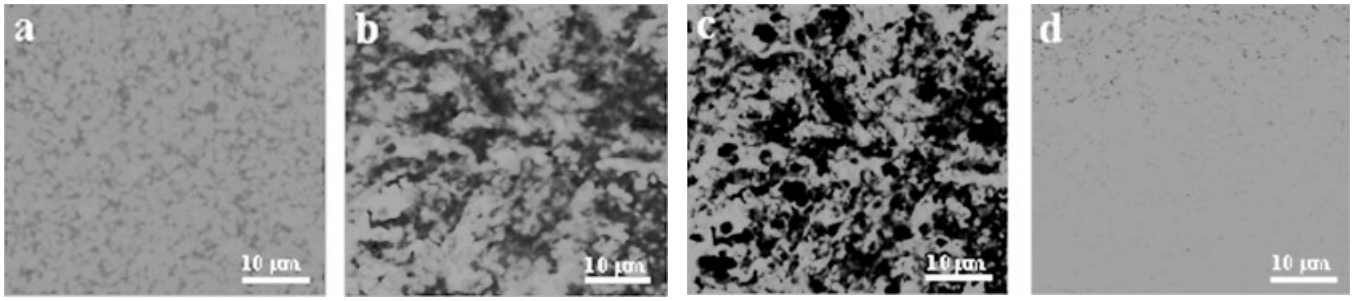

Figure 2. Surface structure of a multilayer film containing PA embedded under twenty (P*l*GA/P*l*L) pairs of layers after incubation with cells, and observed by confocal laser scanning microscopy after: a) 0 min; b) 180 min; and c) 15 h. The terminating layer was formed by FITC-conjugated P*l*L. d) Surface structure of a multilayer film containing PA embedded under twenty (P*d*GA/P*d*L) pairs of layers after incubation with cells overnight.

different x values were followed by quartz crystal microbalance with dissipation (QCMD). We always found a steady decrease in the shifts of the measured quartz resonance frequencies with the number of deposited bilayers, which proves continuous film growth. Treating the data by the viscoelastic model developed by Voinova et al.,[37] we could determine the increase in the film thickness d, as the build-up process went on (Fig. 3). The inset shows the thickness reached by a $(PL/PGA)_6$ film as a function of x. The film thickness depends on the d-content in the build-up solutions. The thickness is approximately symmetric with respect to $x = 50\,\%$, where it goes through a minimum. The change in the film build-up with x shows that the *l*-enantiomers interact differently with *l*- and *d*-enantiomers of the polypeptide of opposite charge. This has already been found by Boulmedais et al.,[38] who investigated the construction of P*d*L/P*l*GA multilayers. They found that the thickness of this film increased more slowly with the number of deposition steps than that of P*l*L/P*l*GA multilayers. This indicates that P*d*L interacts with P*l*GA, but that their interactions are weaker than those of P*l*L with P*l*GA. It is thus also expected that the interactions of P*l*L with P*d*GA are weaker than those of P*d*L with P*d*GA. This could explain the minimum in the film thickness observed for the values of x close to 50 %. Indeed, the difference in the interactions between the *l*- and *d*-enantiomers of polypeptides of opposite sign should lead to some segregation on the surface between *l*- and *d*-poly(lysine)/poly(glutamic acid) complexes. Such a segregation could lead to a decrease in the film thickness. At $x = 50\,\%$, the segregation would be maximum if all the chains have the same mass and mass distribution, and would thus also lead to a minimum in the film thickness.

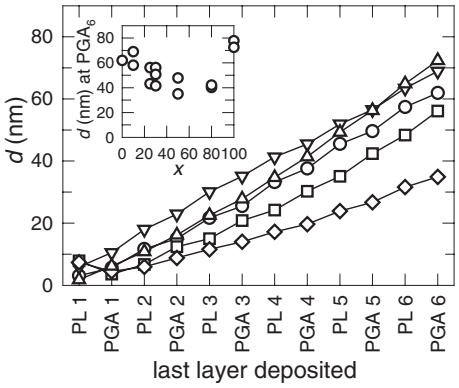

Figure 3. Variation in the thickness of the films, d, as new layers are added for various values of x (0 % (○), 10 % (▽), 30 % (□), 50 % (◇), and 100 % (△). Inset: the thickness of $(PL/PGA)_6$ films as a function of x.

Due to the identical chemical nature of the *l*- and *d*-peptides, we could not determine their ratio in the film. Thus, we shall assume, without loss of generality and just to fix the idea, that the two enantiomers of each polypeptide were incorporated in the film in the same proportion as in the build-up polypeptide solutions.

2.3. Cell Activity

For multilayer films containing embedded PA, the proteins were always adsorbed on a $(PlL/PlGA)_5$-P*l*L precursor film in order to keep the adsorption process (in particular the amount of adsorbed proteins) unaffected by the *d*/*l* composition of the film. The multilayer with a given *d*/*l* composition was then further deposited on top of the $(PlL/PlGA)_5$-P*l*L-PA architecture and consisted of n additional pairs of layers. We always ended the architecture with a poly(lysine) layer in order to promote cell adhesion.[39] These films were then brought into contact with human macrophages for interaction times ranging from one to six hours. The TNF-α production was measured. It was compared to the TNF-α production of a similar film which did not contain PA. Subtracting the second TNF-α production value from the first gives the additional activity due to the presence of PA. These results are gathered in Figure 4.

First, note the good experimental reproducibility for the experiments in which PA was adsorbed on top of the film ($n = 0$) and thus enters in direct contact with the cells. A rapid cellular response was observed after one hour of contact, and it lasted for at least up to six contact hours. For the embedded proteins ($n = 1$, 5, 15, and 20), as a general trend, the TNF-α production decreased when the proportion of *d*-peptides in the film increased. More precisely, when x equaled 50 % or more, the ac-

ADVANCED FUNCTIONAL MATERIALS

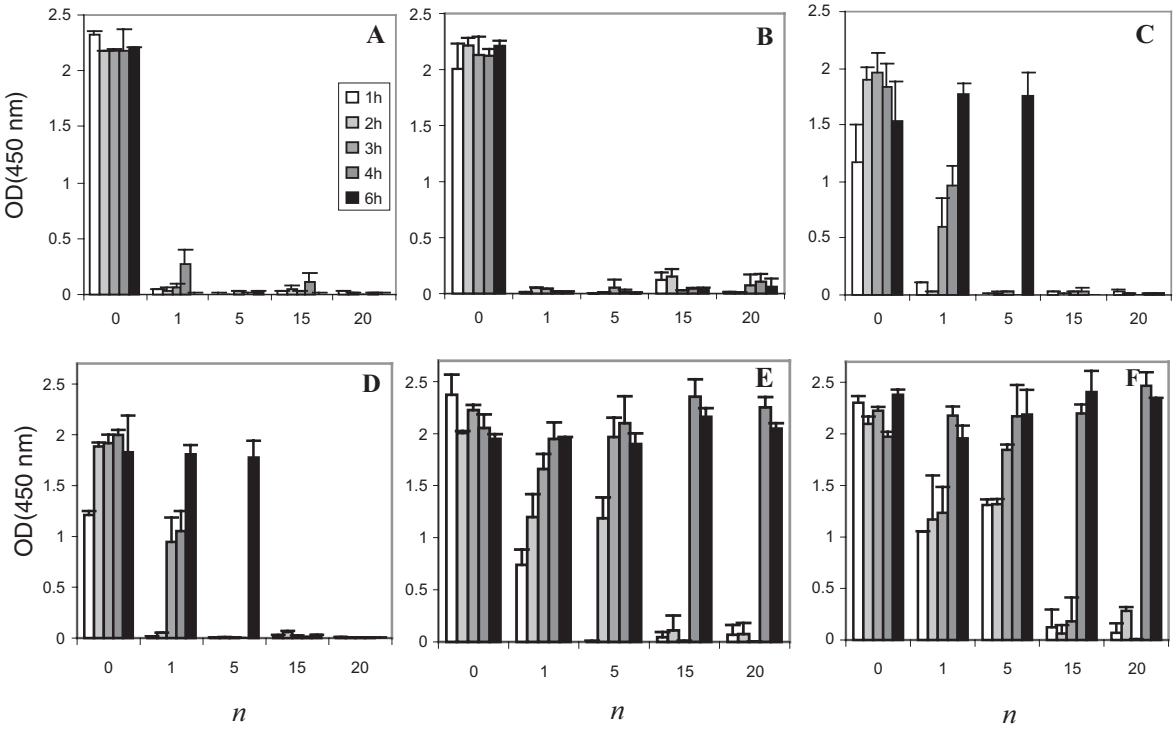

Figure 4. TNF-α secretion by macrophages grown on polyelectrolyte films. Cells were incubated for 1, 2, 3, 4, and 6 h. The height of each bar corresponds to the optical density (OD) at 450 nm, averaged over at least two independent experiments. The error bars represent the standard deviation. The different polyelectrolyte film architectures correspond to: $n=0$, [(P*l*L/P*l*GA)$_5$-P*l*L-PA]; $n=1$, [(P*l*L/P*l*GA)$_5$-P*l*L-PA-(PL/PGA)-PL]; $n=5$, [(P*l*L/P*l*GA)$_5$-P*l*L-PA-(PL/PGA)$_5$-PL]; $n=15$, [(P*l*L/P*l*GA)$_5$-P*l*L-PA-(PL/PGA)$_{15}$-PL]; and $n=20$, [(P*l*L/P*l*GA)$_5$-P*l*L-PA-(PL/PGA)$_{20}$-PL]. The contributions of the P*l*L, P*d*L, P*l*GA, and P*d*GA enantiomers of PL and PGA in the layers constituting the upper part of the films are specified by the value of x indicated in each frame. a) $x=100\,\%$, b) $x=50\,\%$, c) $x=40\,\%$, d) $x=30\,\%$, e) $x=20\,\%$, and f) $x=10\,\%$.

tivity was totally suppressed, even when PA was embedded under a (PL/PGA/PL) trilayer. For x between 0 and 40 %, the biological activity could be finely tuned in time, with a precision of the order of one hour, by adjusting both the *d*-polypeptide content and the embedding depth of the protein. More precisely, for x ranging between 30 and 40 %, the activity gradually increased after two hours of contact when PA was embedded under one layer pair. When embedded under five pairs of layers, the PA activity was totally suppressed during the first four hours, whereas the protein became fully active after six contact hours. Finally, when embedded under fifteen pairs of layers or more, PA no longer acted on cells within the first six hours of contact. For a *d*-content ranging between 10 and 20 %, full activity was observed for all embedding depths up to $n=20$ after four hours of contact between the cells and the film. For embedding depths of up to five pairs of layers, the activity increased continuously with time—a plateau was reached after four contact hours. Finally, when the embedding depth exceeded fifteen pairs of layers, no biological response took place during the initial three hours of contact, but reached its full activity after four hours of contact. This behavior is thus similar to that found for x ranging from 30 to 40 % and an embedding depth of five pairs of layers, but it takes place at shorter times and larger embedding depths. These results clearly demonstrate that the biological activity of the films can be finely tuned on a time scale of about one hour and over at least six hours. A continuously increasing activity, starting as soon as the cells are brought into contact with the film, was obtained by embedding the proteins under a small number of layer pairs. An "off–on" response in time was seen for higher embedding depths—the time at which the biological response turned on increased with the *d*-content of the solution (consequently also of the film architecture).

Now, we return to the total suppression of the biological activity when PA is embedded under a PL/PGA/PL layer with $x=100\,\%$ or $50\,\%$. This unexpected result could be due to either i) the fact that protein A molecules are entirely wrapped with polypeptides, which prevents, for high *d*-content, any interaction between protein A and cells, or ii) the denaturation of protein A by the *d*-polypeptides present in high proportion. Parameters such as the local pH would not be expected to cause this suppression, because the two enantiomers have a similar chemical nature. The second hypothesis (protein denaturation) can be investigated by comparing the Fourier-transform infrared (FTIR) spectra of PA interacting with P*l*L and P*d*L (Fig. 5) and with P*l*GA and P*d*GA in the amide-1 region. In this latter case, the results are similar to those obtained with poly(lysine). The spectra relative to protein A interacting with P*l*L and with P*d*L are indistinguishable. They are also indistinguishable from those obtained by summing the spectra of PA

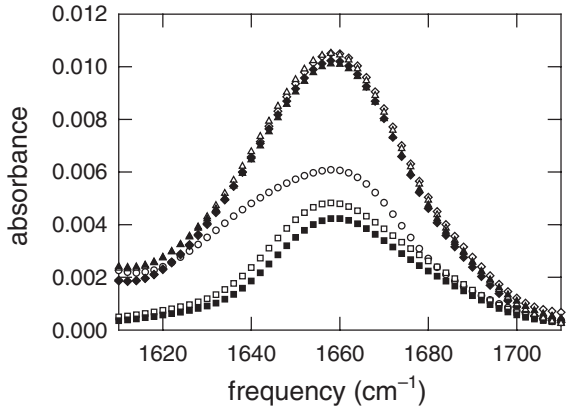

Figure 5. FTIR spectra measured in the transmission mode in the peptide amide-1 region (maximum at 1658 cm^{-1}): PA (○); P*d*L (■); P*l*L (□); complex of P*d*L and PA (◆); complex of P*l*L and PA (◇); sum of PA and P*d*L spectra (▲); and sum of PA and P*l*L spectra (△).

alone and of P*l*L (or P*d*L) alone. This clearly indicates that the interactions between PA and both P*l*L or P*d*L do not affect the secondary structure of protein A. It is thus expected that it is the wrapping of the proteins by a large proportion of *d*-enantiomers that is responsible for the loss of biological activity when embedded close to the top of the film.

We have seen that the film thickness depends upon the *d*/*l* ratio of the build-up polyelectrolyte solutions, and in particular that it decreases as x increases from 0 to 50 %. On the other hand, for a given number of deposited pairs of layers, the biological activity decreases as x increases. The variation in biological effect can thus not be attributed to the change in film thickness with x. The biological effects can rather be explained by a continuous degradation and pseudopod development through the multilayered films,[19] as has already been found on (P*l*L/P*l*GA)$_n$ films. Note that film degradation does not take place in the presence solely of the culture medium: it requires the presence of macrophages. Indeed, CLSM images of films in the presence and absence of the culture medium were taken, and no structural changes were observed: Structural changes were observed in the presence of macrophages (Figs. 2a,c). For films with a high *d*-content ($x \geq 50$ %), this degradation and pseudopod development was not possible within the first six hours. This was confirmed by CLSM: Films containing 50 % of *d*-enantiomer did not show any degradation, even after eight hours of contact, and they looked similar to films constructed with pure *d*-solutions, that is, containing exclusively P*d*GA and P*d*L (Fig. 1d). For small *d*-content films ($x \leq 20$ %), the continuous increase in the film's activity during the first few hours, when PA is embedded under up to five pairs of layers, may result from fluctuations in the *d*- and *l*-content along the multilayer covering the PA layer. This heterogeneity is likely to be responsible for the high variation in the time needed for the pseudopods to enter into contact with PA. For larger embedding depths, PA remains out of reach for a period of time which must correspond to the time needed for the cells to degrade the film down to the PA layer. This time is expected to increase with the embedding depth, as confirmed by our observations. In contrast, what is unexpected is the rapid "off–on" switch effect which takes place over a typical time lapse of the order of one hour, and which was observed when the proteins were embedded under a large number of pairs of layers for $x = 10$ and 20 %, and under five pairs of layers for $x = 30$ and 40 %. This observation could be the consequence of smaller fluctuations of the local *d*-content when the multilayered films consist of more than ten pairs of layers, or when the *d*-content is high. Moreover, it must also be a consequence of the well-defined depth at which the proteins are embedded. This "off–on" switch effect constitutes a very valuable tool for fine tuning the activity of multifunctional films. Note also that, in analogy with P*l*L/P*l*GA films, both poly(lysine) and poly(glutamic acid) should diffuse in and out of the entire multilayer film during its construction. There might be some influence of the diffusion of P*l*L and P*l*GA on the film's degradation. Indeed, degradation of P*l*L (or P*l*GA) could lead to the formation of P*l*L (or P*l*GA) chains of smaller mass. They could then eventually exchange chains of similar nature, but of higher mass, in the film and thus participate to some extent in the film's degradation. This is, however, very difficult to verify experimentally and was not a major issue of this work.

3. Conclusions

We have developed a tool to build-up predefined time-scheduled bioactive films. This was achieved by taking advantage of the great flexibility offered by layer-by-layer deposition technology. Multilayer films were simply constructed using mixtures of degradable and non-degradable polyelectrolyte solutions of known composition. We also took advantage of the ability to incorporate the proteins at very well-defined depths in the film, with a precision of a few tens of nanometers.

4. Experimental

Chemicals: Poly(L-lysine) hydrobromide (P*l*L, weight-average molecular weight, $M_W = 39\,000$ Da), poly(L-lysine) hydrobromide labeled with fluorescein isothiocyanate (P*l*L^{FITC}, $M_W = 23\,000$ Da), poly(D-lysine) (P*d*L, $M_W = 28\,000$ Da, Sigma), poly(D-glutamic acid) (P*d*GA, $M_W = 44\,700$ Da), and poly(L-glutamic acid) (P*l*GA, $M_W = 53\,785$ Da) were purchased from Sigma and used without any further purification. The degree of substitution of P*l*L^{FITC} was 7 mmol FITC per mole of lysine monomer. The *Staphylococcus aureus* PA and PA labeled with sulforhodamine 101 acid chloride (Texas Red) (PA, $M_W = 42\,000$ Da) was from Sigma (Ref: P7837).

Cell Culture: Whole blood samples were purchased from the "Etablissement Français du Sang" (EFS, Strasbourg, France). Peripheral mononuclear blood cells (PBMC) from healthy individuals, seronegative for HIV-1 and hepatitis B and C were isolated from buffy coat by Ficoll/Hypaque centrifugation and were washed twice in phosphate-buffered saline without Ca^{2+}/Mg^{2+}. Monocytes were isolated from whole blood and separated by counter-current centrifugal elutriation of the peripheral mononuclear cells [40]. The purity was measured by flow cytometry staining with fluorochrome antibodies (Becton Dickinson, PharMingen, San Diego, CA) to CD3 (T cells), CD19 (B cells), CD14 (monocytes), and CD45 (leukocytes). Monocytes were diluted at 1.5×10^6 cells mL^{-1} in AIM lymphocytes SVF-free medium with Gluta-

ADVANCED FUNCTIONAL MATERIALS

max, 100 U mL^{-1} (U: unit) GM-CSF (PeproTech, Rocky Hill, USA). The culture medium was changed after three days of culture, and, at day five, the macrophages were washed twice with RPMI (Roswell Parc Memorial Institut) at 37 °C.

Polyelectrolyte Multilayered Film Preparation: Polyelectrolyte multilayers were always prepared on glass coverslips (CML, France) pretreated for 15 min at 100 °C with 10^{-2} M sodium dodecylsulfate (SDS) and 0.12 N HCl, and then extensively rinsed with deionized water. Glass coverslips were deposited in 24-well plates (Nunc, Denmark). All the solutions (polyelectrolyte, PA, and rinsing) used for the film constructions contained 0.15 M NaCl with a pH adjusted to 7.4. At this pH, both poly(lysine) and poly(glutamic acid) are almost fully charged, so they should not form stereocomplexes in solution. The films were constructed with polyelectrolyte (1 mg mL^{-1}) and PA (200 μg mL^{-1}) solutions. The film construction was performed as follows: First, a precursor film consisting of (P*l*L/P*l*GA)$_5$-P*l*L was built. In each deposition step, the surface was brought into contact with the polyelectrolyte solution for 20 min, followed by another contact with the rinsing solution for 5 min. This rinsing step was repeated three times before the adsorption of the polyelectrolyte of opposite charge. After the build-up of the precursor film, PA was adsorbed on the positively charged P*l*L, terminating the precursor film during an overnight contact with PA solution. This film was then rinsed, and the additional (PL/PGA)$_n$-PL film was built using PL and PGA solutions containing (x/100) mg mL^{-1} of P*d*L (P*d*GA) and (1–x/100) mg mL^{-1} of P*l*L (P*l*GA). All the films were then sterilized for 10 min using ultraviolet light (254 nm). Before use, the architectures were put into contact with 1 mL of RPMI without serum for 24 h. It is possible that when the films are brought in contact with the culture medium, their structure and thickness change: The structure of the multilayers is dependent on many different physicochemical parameters [41–43]. However, such changes cannot explain the different biological effects that were observed in this study. Indeed, it is expected that the structure of the P*l*L/P*l*GA multilayers would change in a similar way to the P*d*L/P*d*GA films but, as was shown in this study, the former films show strong biological activity whereas the latter ones do not. Note also that the films were built at room temperature, whereas the experiments with cells were conducted at 37 °C. Previous studies by Boulmedais et al. [38] showed that temperature changes from 20 to 37 °C did not affect the secondary structure of P*l*L/P*l*GA multilayers, and should thus also not greatly affect the structure of our films.

Stimulation Assays: Stimulation assays involving polyelectrolyte films were conducted by seeding 5×10^5 cells (macrophages) onto the PA-containing polyelectrolyte multilayers prepared on glass coverslips and placed into the wells of 24-well plates. TNF-α production by cells was measured by enzyme-linked immunosorbent assay (ELISA). TNF-α levels were detected by an enzyme immunoassay (Endogen Products, Woburn, MA). All experiments were repeated twice and were performed at 37 °C.

Confocal Laser Scanning Microscopy: The films were imaged in liquid conditions using a Zeiss LSM 510 microscope with a ×40/1.4 oil-immersion objective and with 0.4 μm z-section intervals. FITC fluorescence was detected after excitation at 488 nm, cutoff dichroic mirror 488 nm, and emission band-pass filter 505–530 nm (green). Virtual vertical sections were visualized, allowing the thickness of the film to be determined.

Quartz Crystal Microbalance with Dissipation: QCMD (Q-Sense, Göteborg, Sweden) allows the recording of the resonance frequencies of a quartz crystal when a film is deposited on it. In addition, it permits measurement of the dissipation, which is representative of the damping of the crystal oscillations once the excitation electric tension is switched off. Both the resonance frequencies and the dissipation depend on the thickness and the viscoelastic properties of the deposited film. The variation in the thickness of the films along their build-up can be derived from these measurements by processing them with the viscoelastic model developed by Voinova et al. [37].

Fourier-Transform Infrared Spectroscopy in Transmission Mode: Transmission spectra were measured on an EQUINOX 55 spectrophotometer (Bruker, Wissembourg, France) using a DTGS detector. Solutions were poured into a sample cell holder (SPECAC P/N 20510). Transmission spectra were measured using CaF_2 windows. Single-channel spectra from 128 interferograms were calculated between 4000 and 400 cm^{-1}, with 2 cm^{-1} resolution, using Blackman–Harris three-term apodization and Mertz phase correction, with the standard Bruker OPUS/IR software (Version 3.0.4). Each sample (aqueous solution of polypeptide, or PA, or both) was prepared at a concentration of 1 mg mL^{-1} of each component, in a D_2O, 0.15 M NaCl (Prolabo) solution.

Received: March 26, 2004
Final version: August 11, 2004

[1] I. DeScheerder, K. Wang, K. Wilczek, D. Meuleman, R. VanAmsterdam, G. Vogel, J. Piessens, F. Van de Werf, *Circulation* **1997**, *95*, 1549.
[2] C. Hehrlein, A. Arab, C. Bode, *Basic Res. Cardiol.* **1997**, 97, 417.
[3] W. L. Murphy, M. C. Peters, D. H. Kohn, D. J. Mooney, *Biomaterials* **2000**, *21*, 2521.
[4] D. Arcos, C. V. Ragel, M. Vallet-Regi, *Biomaterials* **2001**, *22*, 701.
[5] C. T. Laurencin, M. A. Attawia, L. Q. Lu, M. D. Borden, H. H. Lu, W. J. Gorum, J. R. Lieberman, *Biomaterials* **2001**, *22*, 1271.
[6] Y. Lvov, H. Haas, G. Decher, H. Möhwald, A. Mikhailov, B. Mtchedlishvily, E. Morgunova, B. Vainstein, *Langmuir* **1994**, *10*, 4232.
[7] Y. Lvov, K. Ariga, I. Ichinose, T. Kunitake, *J. Am. Chem. Soc.* **1995**, *117*, 6117.
[8] W. Kong, X. Zhang, M. L. Gao, H. Zhou, W. Li, J. C. Shen *Macromol. Rapid Commun*. **1994**, *15*, 405.
[9] K. C. Dee, T. T. Andersen, R. Bizios, *J. Biomed. Mater. Res.* **1998**, *40*, 371.
[10] J. A. Neff, K. D. Caldwell, P. A. Tresco, *J. Biomed. Mater. Res.* **1998**, *40*, 511.
[11] S. M. Cannizzaro, R. F. Padera, R. Langer, R. A. Rogers, F. E. Black, M. C. Davies, S. J. B. Tendler, K. M. Shakesheff, *Biotechnol. Bioeng.* **1998**, *58*, 529.
[12] Y. Ito, J. Zheng, Y. Imanishi, K. Yonezawa, M. Kasuga, *Proc. Natl. Acad. Sci. USA* **1996**, *93*, 3598.
[13] Y. Ito, G. Chen, Y. Imanishi, *Bioconjugate Chem.* **1998**, *9*, 277.
[14] A. C. R. Grayson, I. S. Choi, P. P. Wang, H. Brem, M. J. Cima, R. Langer, *Nat. Mater.* **2003**, *2*, 767.
[15] G. Decher, *Science* **1997**, *277*, 1232.
[16] N. Jessel, P. Lavalle, F. Meyer, F. Audouin, B. Frisch, P. Schaaf, J. Ogier, G. Decher, J.-C. Voegel, *Adv. Mater.* **2004**, *16*, 1507.
[17] J. Chluba, J.-C. Voegel, G. Decher, P. Erbacher; P. Schaaf, J. Ogier. *Biomacromolecules* **2001**, *2*, 800.
[18] N. Jessel, P. Schwinté, P. Falvey, R. Darcy, Y. Haïkel, P. Schaaf, J.-C. Voegel, J. Ogier, *Adv. Funct. Mater.* **2004**, *14*, 174.
[19] N. Jessel, F. Atalar, P. Lavalle, J. Mutterer, G. Decher, P. Schaaf, J.-C. Voegel, J. Ogier, *Adv. Mater.* **2003**, *15*, 692.
[20] J. D. Mendelsohn, S. Y. Yang, J. Hiller, A. I. Hochbaum, M. F. Rubner, *Biomacromolecules* **2003**, *4*, 96.
[21] Y. Lvov, H. Haas, G. Decher, H. Möhwald, A. Mikhailov, B. Mtchedlishvily, E. Morgunova, B. Vainstein, *Langmuir* **1994**, *10*, 4232.
[22] W. Kong, L. P. Wang, M. L. Gao, H. Zhou, X. Zhang, W. Li, J. C. Shen, *J. Chem. Soc., Chem. Commun.* **1994**, 1297.
[23] G. Ladam, P. Schaaf, F. Cuisinier, G. Decher, J.-C. Voegel, *Langmuir* **2001**, *17*, 878.
[24] F. Caruso, K. Niikura, D. N. Furlong, Y. Okahata, *Langmuir* **1997**, *13*, 3427.
[25] P. Schwinté, J.-C. Voegel, C. Picart, Y. Haikel, P. Schaaf, B. Szalontai, *J. Phys. Chem. B* **2001**, *105*, 11 906.
[26] S. Kumar, Y. Shukla, A. K. Prasad, A. S.Verma, P. D. Dwividi, N. K. Mehrotra, P. K. Ray, *Cancer Lett.* **1992**, *61*, 105.
[27] A. S. Verma, P. D. Dwivedi, A. Mishra, P. K. Ray, *Int. Immunopharmacol.* **1999**, *21*, 89.
[28] V. Subbulakshmi, A. K. Ghosh, T. Das, P. K. Ray, *Biochem. Biophys. Res. Commun.* **1998**, *2*, 50.
[29] P. K. Ray, S. Raychaudhury, P. Allen, *Cancer Res.* **1982**, *42*, 4970.

[30] A. K. Srivastava, K. P. Singh, P. K. Ray, *Mycopathologia* **1997**, *138*, 21.
[31] A. C. Ghose, A. Mookerjee, K. Sengupta, A. K. Ghosh, S. Dasgupta, P. K. Ray, *Immunol. Lett.* **1999**, *65*, 175.
[32] M. Frankenberger, H. Pechumer, H. W. Ziegler-Heitrock, *J. Inflammation* **1995**, *45*, 56.
[33] S. Leporatti, C. Gao, A. Voight, E. Donath, H. Möhwald, *Eur. Phys. J. E* **2001**, *5*, 13.
[34] Z. Sui, J. B. Schlenoff, *Langmuir* **2003**, *19*, 7829.
[35] M. Debreczeny, V. Ball, F. Boulmedais, B. Szalontai, J.-C. Voegel, P. Schaaf, *J. Phys. Chem. B* **2003**, *107*, 12 734.
[36] E. Hübsch, V. Ball, B. Senger, G. Decher, J.-C. Voegel, P. Schaaf, *Langmuir* **2004**, *20*, 1980.
[37] M. V. Voinova, M. Rodahl, M. Jonson, B. Kasemo, *Phys. Scr.* **1999**, *59*, 391.
[38] F. Boulmedais, M. Bozonnet, P. Schwinté, J.-C. Voegel, P. Schaaf, *Langmuir* **2003**, *19*, 9873.
[39] L. Richert, Ph. Lavalle, D. Vautier, B. Senger, J.-F. Stoltz, P. Schaaf, J.-C. Voegel, C. Picart, *Biomacromolecules* **2002**, *3*, 1170.
[40] P. K. Lund, G. B. Joo, A. B. Westvik, R. Ovstebo, P. Kierulf, *J. Immunol. Methods* **1988**, *112*, 213.
[41] J. D. Mendelsohn, C. J. Barrett, V. V. Chan, A. J. Pal, A. M. Mayes, M. F. Rubner, *Langmuir* **2000**, *16*, 5017.
[42] S. T. Dubas, J. B. Schlenoff, *Langmuir* **2001**, *17*, 7725.
[43] S. T. Dubas, J. B. Schlenoff, *Macromolecules* **2001**, *34*, 3736.

